


RESEARCH ARTICLE

Relevance of VEGF and CD147 in different SARS-CoV-2 positive digestive tracts characterized by thrombotic damage

Daria Bortolotti¹ | Carolina Simioni^{2,3} | Luca Maria Neri^{3,4} | Roberta Rizzo¹ | Chiara Marina Semprini^{4,5} | Savino Occhionorelli^{4,6} | Ilaria Laface⁴ | Juana Maria Sanz¹ | Giovanna Schiuma¹ | Sabrina Rizzo¹ | Gabriele Varano⁴ | Silvia Beltrami¹ | Valentina Gentili¹ | Roberta Gafà^{4,7} | Angelina Passaro^{4,5} 

¹Department of Chemical and Pharmaceutical Sciences, University of Ferrara, Ferrara, Italy

²Department of Life Sciences and Biotechnology, University of Ferrara, Ferrara, Italy

³Laboratory for Technologies of Advanced Therapies (LTTA)-Electron Microscopy Center, University of Ferrara, Ferrara, Italy

⁴Department of Translational Medicine, University of Ferrara, Ferrara, Italy

⁵Medical Department, University Hospital of Ferrara Arcispedale Sant'Anna, Ferrara, Italy

⁶Surgery Department, University Hospital of Ferrara Arcispedale Sant'Anna, Ferrara, Italy

⁷Oncological and Medical Department, University Hospital of Ferrara Arcispedale Sant'Anna, Ferrara, Italy

Correspondence

Angelina Passaro, Department of Translational Medicine, University of Ferrara, Via Luigi Borsari, 46 - 44121 Ferrara, Italy.
Email: angelina.passaro@unife.it

Roberta Rizzo, Department of Chemical and Pharmaceutical Sciences, University of Ferrara, Via Luigi Borsari, 46 - 44121, Ferrara, Italy.
Email: roberta.rizzo@unife.it

Funding information

This study was supported by COVID-19 grant from the University of Ferrara (PI: Roberta Rizzo and Angelina Passaro) and by crowdfunding campaign from University of Ferrara (PI Daria Bortolotti).

Abstract

Several evidence suggests that, in addition to the respiratory tract, also the gastrointestinal tract is a main site of severe acute respiratory syndrome CoronaVirus 2 (SARS-CoV-2) infection, as an example of a multi-organ vascular damage, likely associated with poor prognosis. To assess mechanisms SARS-CoV-2 responsible of tissue infection and vascular injury, correlating with thrombotic damage, specimens of the digestive tract positive for SARS-CoV-2 nucleocapsid protein were analyzed deriving from three patients, negative to naso-oro-pharyngeal swab for SARS-CoV-2. These COVID-19-negative patients came to clinical observation due to urgent abdominal surgery that removed different sections of the digestive tract after thrombotic events. Immunohistochemical for the expression of SARS-CoV-2 combined with a panel of SARS-CoV-2 related proteins

Abbreviations: ac, adsorption cells; ACE2, angiotensin-converting enzyme 2; acm, apical cell membrane; CD147, cluster of differentiation 147; COVID-19, coronavirus disease 2019; csg, cytoplasmic secretory granules; e, erythrocytes; gc, glycocalyx; GCs, goblet cells; HLA-E, human leukocyte antigen-E; HLA-G, human leukocyte antigen-G; HLA-I, human leukocyte antigen class-I; IHC, immunohistochemical; MMP-9, matrix metalloproteinase-9; NP, nucleocapsid protein; SARS-CoV-2, severe acute respiratory syndrome CoronaVirus 2; SP, spike protein; TEM, transmission electron microscopy; VEGF, vascular endothelial growth factor.

Daria Bortolotti and Carolina Simioni contributed equally to this article and both should be considered first author.

Luca Maria Neri and Roberta Rizzo contributed equally to this article and both should be considered second author.

Roberta Gafà and Angelina Passaro contributed equally to this article and both should be considered senior author.

angiotensin-converting enzyme 2 receptor, cluster of differentiation 147 (CD147), human leukocyte antigen-G (HLA-G), vascular endothelial growth factor (VEGF) and matrix metalloproteinase-9 was performed. Tissue samples were also evaluated by electron microscopy for ultrastructural virus localization and cell characterization. The damage of the tissue was assessed by ultrastructural analysis. It has been observed that CD147 expression levels correlate with SARS-CoV-2 infection extent, vascular damage and an increased expression of VEGF and thrombosis. The confirmation of CD147 co-localization with SARS-CoV-2 Spike protein binding on gastrointestinal tissues and the reduction of the infection level in intestinal epithelial cells after CD147 neutralization, suggest CD147 as a possible key factor for viral susceptibility of gastrointestinal tissue. The presence of SARS-CoV-2 infection of gastrointestinal tissue might be consequently implicated in abdominal thrombosis, where VEGF might mediate the vascular damage.

KEYWORDS

CD147, digestive tract, inflammation, SARS-CoV-2, thrombosis

1 | INTRODUCTION

Symptomatic coronavirus disease 2019 (COVID-19) patients have been commonly identified as individuals who developed signs and symptoms suggestive of COVID-19. Even if epidemiology and virological studies suggest that virus transmission from an infected person mainly occur from respiratory tract through direct droplet and aerosol transmission,¹ also respiratory asymptomatic infections play an important role in infection spread and clinical outcome.²

As already reported,³ evidences suggest that severe acute respiratory syndrome CoronaVirus 2 (SARS-CoV-2) may replicate inside various cell types and tissues besides the lung, including the gastrointestinal tract, suggesting intestine as a main site of SARS-CoV-2 infection.³

The ability of SARS-CoV-2 to infect a broad spectrum of tissues could be imputed to the diffuse tissue expression of SARS-CoV-2 cellular receptor angiotensin-converting enzyme 2 (ACE2),⁴ which regulates blood pressure, fluids, electrolyte balance and systemic vascular resistance.^{4,5}

ACE2 was established as the functional host receptor for SARS-CoV-2,⁶ and its presence could confer susceptibility to host cell entry of the virus.

Besides ACE2, other molecules seem to participate in SARS-CoV-2 infection,⁷ including several molecules that might be involved in SARS-CoV-2 cell susceptibility, such as Neuropilin 1 and cluster of differentiation 147 (CD147), cyclophilin A, reported to be associated with enhanced viral infection.⁸⁻¹²

CD147 is expressed in a wide range of tissues, including lungs and intestinal vascular endothelium,¹³ where it plays a role in the control of intestinal inflammation.¹⁴ CD147 expression is increased during pathological conditions in the lung,

bowel tissues,¹³ and during stroke.¹⁵ Recent studies described a possible interaction between CD147 binding site and SARS-CoV-2 spike protein (SP) receptor-binding domain by electrostatic interactions involving the residues Arg403, Asn481, and Gly502.¹⁶ The treatment with Meplazumab, an anti-CD147 humanized antibody, is able to inhibit SARS-CoV-2 infection.⁸ Again, Fenizia et al., have reported that CD147 binding to cyclophilin A does not play a role in SARS-CoV-2 entry, but CD147 regulates ACE2 levels and both receptors are affected by virus infection, supporting a possible CD147 involvement in SARS-CoV-2 infection.¹⁷ Anyway, controversial results were reported with no evidence for a direct SARS-CoV-2 spike binding for CD147.¹⁸ This is suggestive of a possible role of CD147 as a susceptibility factor for SARS-CoV-2 infection that might cooperate with SARS-CoV-2 specific receptors. In particular, CD147 expression has been reported on vascular endothelium in the absence of ACE2, underlying the potential implication of this molecules in vascular damages due to SARS-CoV-2 infection, independently from ACE2 presence.¹⁹

In this view, the engagement of both ACE2 and CD147 by SARS-CoV-2 may explain the vascular damage and thrombosis associated to excessive inflammation observed in COVID-19 patients.²⁰ The detrimental effect of SARS-CoV-2 infection at vascular level is also confirmed by the elevated vascular endothelial growth factor (VEGF) levels found in COVID-19 patients.²¹

Despite SARS-CoV-2 infection triggers to cytokine-storm process in COVID-19 patients,²² the host immune system could not efficiently counteract the infection.²³ It is known that viruses may induce the expression of immunomodulatory non-classical human leukocyte antigen class-I molecules,²⁴ such as human leukocyte antigen-E²⁵ and human leukocyte antigen-G (HLA-G).²⁶ HLA-G controls the immune

system activation by interacting with specific inhibitory receptors expressed on immune cells.²⁷ HLA-G immunomodulatory function is exploited by viruses as an immune-escape mechanism,^{28,29} and has recently reported in SARS-CoV-2 gastroenteric infection,³ suggesting a role of HLA-G in gastrointestinal pathogenetic mechanisms in COVID-19.

Another regulator of the COVID-19 inflammatory process is represented by matrix metalloproteinases-9 (MMP-9), which is considered an early indicator of respiratory failure³⁰ and has been also reported as involved in the modulation of inflammation in intestinal pathological conditions.³¹ Moreover, MMPs are known to be involved in HLA-G cleavage³² and, in particular, MMP-9 is known to be upregulated in lung macrophages via CD147,^{15,33,34} together with VEGF increase in bowel disease.

In this study, the presence of SARS-CoV-2 infection was investigated in digestive tract tissues specimens obtained from three SARS-CoV-2 tested negative patients that underwent abdominal surgery for acute abdominal symptoms and that presented a clinical history very suspicious for COVID-19 infection. Tissues were evaluated for the expression of SARS-CoV-2 nucleocapsid protein (NP), ACE2, CD147, HLA-G, VEGF, and MMP-9. Moreover, transmission electron microscopy (TEM) analyses were performed in order to characterize morpho-functional alterations.

2 | MATERIAL AND METHODS

The study adheres to the ethical principles for medical research involving human subjects as required by the 2013 revision of the Declaration of Helsinki—WMA Declaration of Helsinki—Ethical Principles for Medical Research Involving Human Subjects.

The study was structured in accordance with the STROBE guidelines for observational studies and STROME-ID for reporting of molecular epidemiology for infectious diseases. It was evaluated by the Ethics Committee of the Area Vasta Emilia Centro della Regione Emilia-Romagna (CE-AVEC) with the number 122/2021/Oss/AOUFe.

2.1 | Patients

Three patients (1 female and 2 male) aged 64–76 presenting with acute abdominal symptoms were respectively submitted to ileum and gallbladder surgical resection (patient 1), sigmoidectomy (patient 2), and duodenal-jejunum tract resection (patient 3) at the Department of Surgical Emergencies at the University Hospital of Ferrara (Italy). On admission, patients did not show any usual clinical signs of COVID-19. Patient clinical characteristics are reported in Table 1.

During hospitalization, patients performed multiple times oro/naso-pharyngeal swabs resulting always negative for SARS-CoV-2. All the surgical specimens were collected and routinely processed at the Pathology Lab.

2.2 | Immunohistochemical analysis

Immunohistochemical (IHC) analysis was performed on the collected samples for detection of SARS-CoV-2 NP (NB100-56576, Novus Biologicals, Centennial, 1:250 dilution), HLA-G antibody (MEM-G2, Exbio, dilution 1:400), CD147 (clone MEM-M6/1, dilution 1:100, Novus Biologicals), ACE2 (clone EPR4435-2, 1:250 dilution, Abcam), VEGF-A (VG-1, 5 µg/ml concentration, Abcam), MMP9 (clone EP1254, 1:1000 dilution, Abcam). Slides were counterstained with H-E. Specificity for SARS-CoV-2 staining was investigated performing SARS-CoV-2 NP IHC analysis on samples obtained from a non COVID-19 patient, as described previously³ (Figure S1).

2.3 | Evaluation of SARS-CoV-2 SP binding and CD147 expression on bowel tissues

SARS-CoV-2 SP binding and CD147 expression was evaluated on bowel samples from non-COVID-19 patients by IHC analysis.^{35,36} Briefly, tissue slides were incubated with trimeric full-length SARS-CoV-2 SP (1 µg/ml, AcroBiosystems) for 1 h at RT, in order to allow protein-receptor binding, and then incubated with SARS-CoV-2 SP antibody (dilution 1:400, SinoBiological) for detection. The same experiment was performed also adding CD147 antibody (clone MEM-M6/1, dilution 1:100, Novus Biologicals), following the ImmPRESS Duet Double Staining Polymer Kit (Vector Laboratories) protocol to visualize SARS-CoV-2 SP and CD147 co-localization.

2.4 | Cell lines

Human colorectal adenocarcinoma Caco-2 cell line (ATCC HTB-37) was grown in EMEM medium with 1% L-glutamine, 1% Penicillin/Streptomycin and 20% FBS. Vero E6 cells (ATCC CRL-1586) were grown in EMEM medium with 1% L-glutamine, 1% Penicillin/Streptomycin, and 10% FBS.

2.5 | SARS-CoV-2 infection and viral RNA detection

SARS-CoV-2, a kind gift of Professor Arnaldo Caruso from University of Brescia, was isolated from a nasopharyngeal

TABLE 1 Patient's clinical characterization

Patients	Sex, age	Relevant clinical features	Symptoms ad admission	Biological parameters
Patient 1	F, 76	Hypercholesterolemia, heavy smoker, mastectomy for breast cancer 30 years previously No chronic therapy	Abdominal pain and vomiting Abdominal CT showed on an atherosclerotic plaque in proximity of the celiac trunk, abdominal fluid accumulation and distended, radiologically heterogeneous, gallbladder (no gallstones), surrounded by fluid She died at home 4 months later	White blood cells $15.76 \times 10^3/\mu\text{l}$, lactate dehydrogenase 293 U/L
Patient 2	F, 64	None No chronic therapy	Severe abdominal pain	Hemoglobin 8.6 g/dl, white blood cells $1.20 \times 10^3/\mu\text{l}$, D-dimer 4.4 $\mu\text{g}/\text{ml}$, C-reactive protein 32 mg/dl, Troponin I 448 ng/L, B-type natriuretic peptide 230 pg/ml
Patient 3	M, 79	Coronary heart disease and dilated ventricular apex Treated with warfarin	Abdominal pain and high fever	Hemoglobin 8.6 g/dl, White blood cells $1.40 \times 10^3/\mu\text{l}$, Procalcitonin 79 ng/ml, C-reactive protein 25 mg/dl, Prothrombin time 4.16 s, D-dimer 3.38 $\mu\text{g}/\text{ml}$

swab retrieved from a patient with COVID-19 (Caucasian man of Italian origin, genome sequences available at GenBank - SARS-CoV-2-UNIBS-AP66: ERR4145453).³⁷ This SARS-CoV-2 isolate clustered in the B1 clade which includes most of the Italian sequences, together with sequences derived from other European countries and United States. The identity of the strain was verified in Vero E6 cells using real-time polymerase chain reaction (PCR) and metagenomic sequencing, from which the reads were mapped to nCoV-2019 (genomic data are available at EBI under study accession no. PRJEB38101). We propagated the clinical isolate in Vero E6 cells and determined the viral titer using a standard plaque assay. Caco-2 cells were infected with a multiplicity of infection (MOI) of 0.05 for 1 h at 37°C. RNA extraction was performed 24 h post infection (hpi) as described previously²⁵ by using MagMAX Viral/Pathigen Nuclei Acid Isolation kit (ThermoFisher, Italy) according to the manufacturer's instructions. SARS-CoV-2 titration by RealTime-PCR was performed with the TaqMan 2019nCoV assay kit v1 (ThermoFisher, Italy).

2.6 | ACE2 and CD147 blocking assay

ACE2 and CD147 blocking was performed in Caco-2 cells using the specific neutralizing antibodies Anti-ACE2 (human) mAb blocking (AC384) (AdipoGen; USA) and

the CD147 Monoclonal Antibody (RL73), Functional Grade (eBioscience; USA). Briefly, Caco-2 cells were incubated with the neutralizing antibodies (alone or in combination) at the concentration of 0.5 $\mu\text{g}/\text{ml}$ for 1 h, before SARS-CoV-2 infection. Then, cells were infected with SARS-CoV-2 inoculum at a MOI of 0.05 and RNA was collected for viral titration, as described above.

2.7 | Transmission electron microscopy

For TEM analysis, samples were fixed in 2.5% glutaraldehyde in 0.1 M phosphate buffer pH 7.4 and post-fixed in 2% osmium tetroxide, dehydrated in acetone solutions and included in Araldite Durcupan ACM (Fluka). Samples were then counterstained with uranyl acetate in saturated solution and lead citrate and observed under transmission electron microscope Zeiss EM910 at 100 kv. Duodenal and colon samples obtained from non-COVID-19 patients were also analyzed to compare the results.

2.8 | Statistical analysis

IHC slide images were analyzed using QuPath software for evaluation of cell percentage positivity and H-Score for each antigen investigated.

An H-score between 0 and 300 was obtained where 300 was equal to 100% of cells strongly stained (3+). Frequencies were analyzed by Chi-square test and H-Score comparisons were evaluated by Student t-test. The statistical analysis was performed by GraphPad Software.

3 | RESULTS

3.1 | Digestive tract showed a differential susceptibility to SARS-CoV-2 infection

The analysis of specimens from gallbladder, ileum, duodenal-jejenum tract, and colon resections evidenced a different distribution of SARS-CoV-2 infection (Figure 1). As showed in Figure 1A–D, the highest presence of SARS-CoV-2 infection was found in gallbladder from patient 1 (Figure 1B) and in colon from patient 2 (Figure 1C). Considering the percentage of positive cells for SARS-CoV-2 NP, there was a significant difference among the four tissues analyzed (Figure 2A), with the highest frequency of positive cells in the gallbladder from patient 1 ($p < .0001$). This trend was confirmed also in terms of the amount of viral presence expressed as H-Score (Figure 2B, $p < .01$ and $p < .001$). Interestingly, considering patients 1, a different distribution between gallbladder and ileum was observed, supporting the evidence of a different susceptibility to SARS-CoV-2 infection of the two tissues (Figures 1A,B and 2A,B).

3.2 | CD147 expression and SARS-CoV-2 gastrointestinal infection

The four specimens were then investigated for the expression of ACE2 and CD147 surface molecules. The IHC analyses (Figure 1E–H) revealed that ACE2 is expressed in all the tissues, except for the colon sample from patient 2 (Figure 1G), as confirmed also by evaluation of positive cell percentage (Figure 2A, $p < .0001$ Chi-square test) and by H-Score (Figure 2C; $p < .05$ and $p < .001$). This result was very controversial, since a consistent presence of infection in the colon sample from patient 2 was reported (Figure 1C). The IHC analysis for CD147 (Figure 1I–L) showed the highest expression in patient 1 gallbladder (Figure 1J), while mild expression in the colon of patient 2 (Figure 1K) and a low expression in ileum of patient 1 and in duodenum of patient 3 (Figure 1I,L) was found respectively, as confirmed by positive cell percentage (Figure 2A, $p < .0001$) and H-Score (Figure 2D; $p < .01$) analysis. The increased expression of CD147 observed in gallbladder from patient 1 (Figure 1J) and in colon from patient 2 (Figure 1K) correlates with the amount of SARS-CoV-2 infection detected in these two samples, suggesting CD147 as crucial in SARS-CoV-2 cell entry at the digestive tract level, despite ACE2 expression. This observation is strengthened by the different expression of CD147 found in ileum and gallbladder samples from patient 1 (Figure 1I,J), in contrast with the comparable expression of ACE2 in the two samples (Figure 1E,F), where a correlation between high

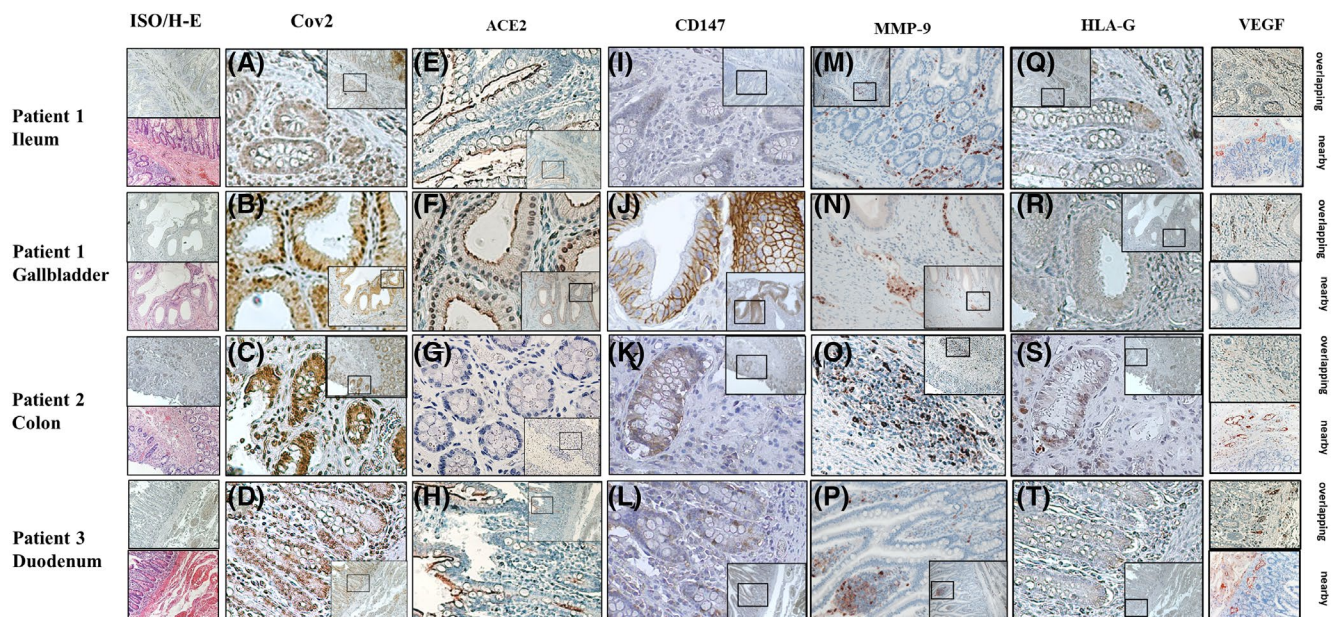


FIGURE 1 Biopsies immunohistochemical analysis. Patient 1 ileum (upper line panels) and gallbladder (second line panels), Patient 2 colon (third line panels) and Patient 3 ileum (bottom panels) were stained for SARS-CoV-2 NP (Cov-2, A–D); ACE2 (E–H), CD147 (I–L), MMP-9 (M–P), HLA-G (Q–T), and for VEGF (right column panels) at site of infection (overlapping) or in an adjacent area (nearby). Samples were also stained with control isotype and with Hematoxylin-Eosin staining (left column panels). Images magnification is 20× or 40×

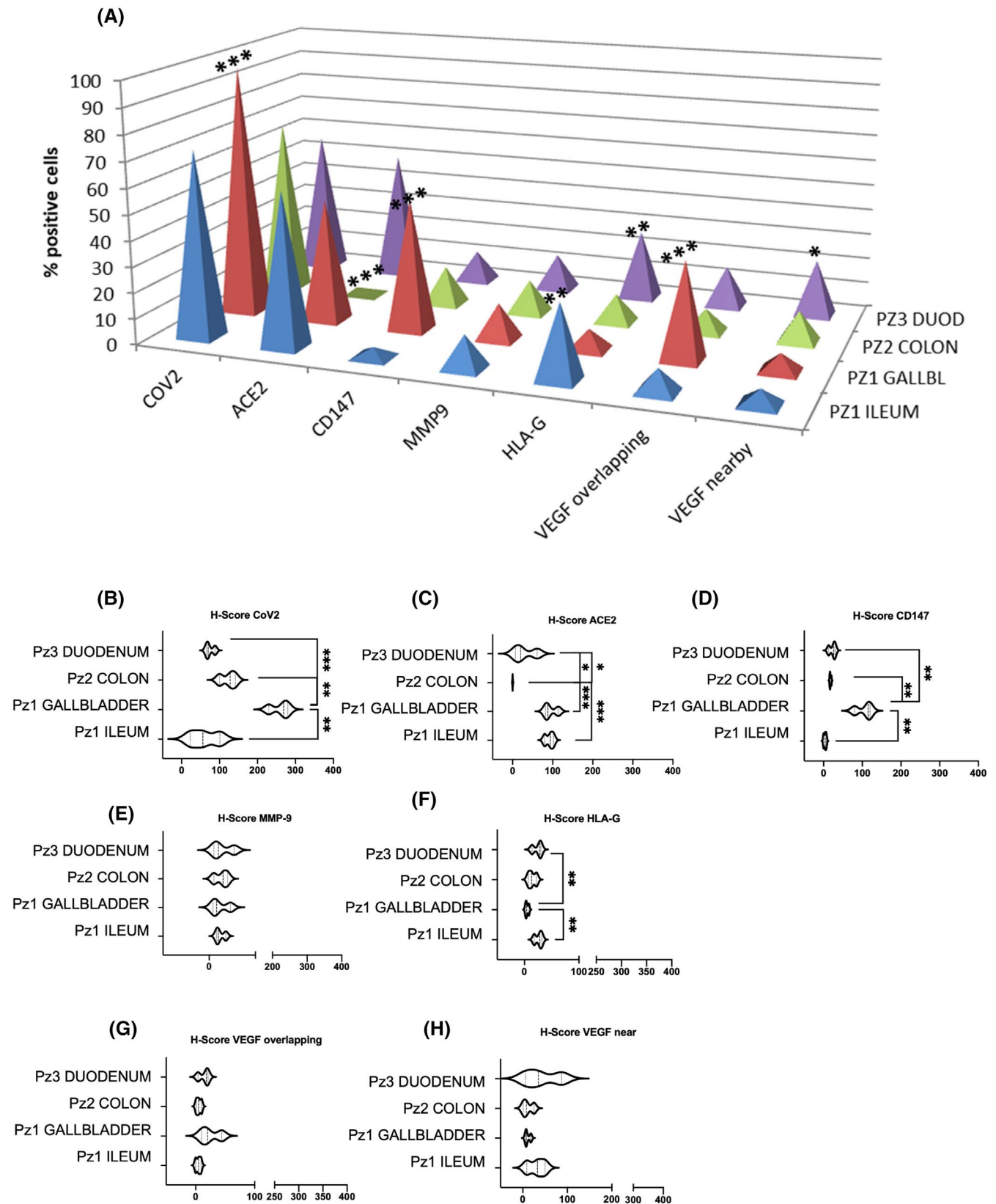


FIGURE 2 Evaluation of sample staining by QuPath software. All the antigens investigated by IHC analysis in tissue biopsies were evaluated by QuPath software for positive cell percentage (A) and for H-Score (B–H) for each antigen (SARS-CoV-2 NP (B), ACE2 (C) CD147 (D), MMP-9 (E), HLA-G (F) VEGF overlapping (G), and nearby (H) the site of infection)

CD147 expression and presence of SARS-CoV-2 has been found in the gallbladder, but not in the ileum.

3.3 | MMP-9 expression during SARS-CoV-2 infection is independent from viral entry

Tissue samples were then stained for MMP-9, which has been described associated to lung function reduction in COVID-19 patients.³⁰ MMP-9 expression was found in all the samples analyzed (Figures 1M–P and 2A,E), with no significant differences. This result suggests that, contrary to what has been observed in the lungs, MMP-9 expression in the digestive tract is not involved in the pathogenic process associated to the virus.

3.4 | SARS-CoV-2 digestive tract infection modulates HLA-G expression and shedding via CD147

HLA-G expression at gut level has been reported to be modulated by SARS-CoV-2 as a mechanism of immune-escape.³

The analysis for the presence of HLA-G in the four tissue samples reported a low-mild expression in patient 1 ileum, patient 2 colon and patient 3 duodenum (Figure 1Q,S,T), while a significant lower HLA-G expression was found in the gallbladder from patient 1 (Figure 1R) in terms of both cell percentage (Figure 2A, $p < .001$) and H-Score (Figure 2F, $p < .01$). Since HLA-G is not normally expressed at the digestive tract level, the reported presence of the molecule seems to confirm its role in SARS-CoV-2 immune-escape. Furthermore, HLA-G expression inversely correlate with CD147, suggesting that the ability of CD147 to also modulate other MMPs than MMP-9³⁸ may contribute to HLA-G membrane shedding.³² Possibly, the high expression of CD147 (Figure 1J) reported in gallbladder, but not in the ileum, from patient 1, could be responsible for the loss of HLA-G observed via CD147/MMPs induction on the gallbladder sample.

3.5 | SARS-CoV-2 digestive tract infection leads to venous thrombotic event via VEGF

In order to evaluate the possible correlation between SARS-CoV-2 infection and abdominal damage associated to thrombosis, all samples were evaluated for VEGF expression in the same areas which SARS-CoV-2 IHC reactivity was demonstrated (Figure 1 overlapping) and also in the adjacent area (Figure 1 nearby). An increased VEGF

expression was found in areas with SARS-CoV-2 presence in patient 1 gallbladder (Figure 1 overlapping), showing statistical significance considering the percentage of positive cells (Figure 2A, $p < .00001$), but not in terms of H-Score (Figure 2G), even if patients 2 gallbladder showed higher score compared with the other samples.

Concerning VEGF expression in the infection adjacent area (Figure 1 nearby), patient 3 duodenum showed the highest percentage of VEGF positive cells (Figures 1 and 2, $p = .0014$) and the highest H-Score (Figure 2H), without reaching significance.

These data suggested a role of the virus in inducing VEGF expression, possibly facilitating the onset of the venous thrombotic event. This is even more evident concerning patient 1 gallbladder, where the expression of VEGF is associated to a notable SARS-CoV-2 presence (Figure 1B).

3.6 | SARS-CoV-2 SP binding-site co-localizes with CD147 expression in gastrointestinal tissues

We evaluated the possible co-localization of SARS-CoV-2 SP binding-site and CD147 expression in bowel tissues of SARS-CoV-2-negative samples.

As shown in Figure 3, SARS-CoV-2 SP is able to bind bowel tissues as gallbladder and ileum in the proximity of sites where CD147 is expressed. The double staining assay showed a co-localization of CD147 and SP proteins, that supports a possible CD147 involvement in viral infection in gastrointestinal tissues.^{16,17}

As a proof of concept, we analyzed the role of CD147 in SARS-CoV-2 infection of epithelial intestinal cells. Caco-2 cell line was infected with SARS-CoV-2, and the viral load was evaluated by quantitative reverse-transcription PCR. We confirmed that Caco-2 cell line is permissive to SARS-CoV-2 infection (Figure 4A). Since Caco-2 cells express both ACE2 and CD147 receptors¹⁴ we blocked both of them to evaluate their role in SARS-CoV-2 infection of epithelial intestinal cells. The blocking of the ACE-2 receptor reduced the viral load (Figure 4B). Interestingly, the blocking of CD147 reduced drastically SARS-CoV-2 infection of Caco-2 cells, similarly to ACE-2/CD147 blocked cells (Figure 4B). These results, in an in vitro setting, suggest a role of CD147 in SARS-CoV-2 infection of epithelial intestinal cells.

3.7 | SARS-CoV-2 infection induces morphological changes in the digestive tract

TEM analysis was performed in order to characterize morpho-functional alterations and differences of the

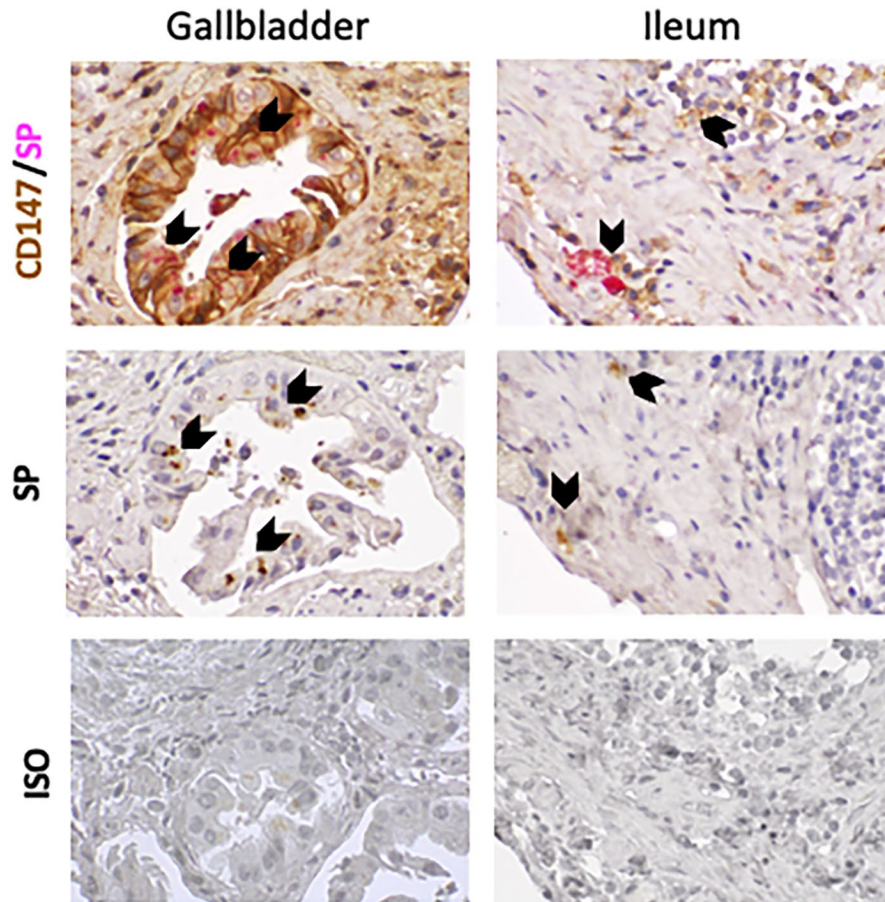


FIGURE 3 Evaluation of SARS-CoV-2 Spike Protein (SP) binding-site and to CD147 co-localization in non-COVID19 bowel samples by IHC analysis. The upper panel reports the double IHC staining for SP (magenta) and CD147 (brown); the middle panel shows the SP (brown) binding to the tissues (ileum and gallbladder); the lower panel represents tissue staining for Isotype control. Black arrows indicate SARS-CoV-2 SP-CD147 co-localization. Magnification 60×

three patient tissues. A significantly different morphological gut microvilli profile was revealed. A colon sample and a duodenal sample from non-COVID-19 patients showed the well organized and aligned microvilli, with a regular distribution protruding from the apical cell membrane (acm) and a homogeneous glycocalyx (gc) (Figure 5A–D). In the colon of patient 2 and in the duodenum of patient 3 microvilli displayed a shorter length than the normal condition, they were severely damaged and, in the colon, a section appears detached from the epithelium (Figure 5E–H). It was not possible to evaluate the morphological state of the ileum of patient 1 as the tissue appeared completely haemorrhagic (data not shown).

Subsequently, for the three patients, the apical region and the lamina propria were also analyzed. Patient 1 ileum presented a high inflammation status and it was not possible to appreciate the morphology of the components of the intestinal epithelium. In particular, in both acquisitions a significant number of erythrocytes (e) can be seen (Figure S2A,B). In patients 2 and 3 samples, cytoplasmic rarefaction accompanied by an overall disintegration of the various cellular components, can generally be observed. In patient 2 colon sample goblet cells can be appreciated, as well as cytoplasmic secretory granules,

adsorption cells, and mucus granules are shown in the duodenum of patient 3 (Figure S2C–F).

4 | DISCUSSION

Concerning COVID-19, the presence of a peculiar intestinal pathological condition has not been reported previously, although the intestinal infarct represents an interstitial pneumonia complication in positive COVID-19 patients.^{39,40}

In this work, digestive tract specimens obtained from three persistently SARS-CoV-2-negative patients that underwent abdominal surgery for acute abdominal symptoms and that presented a clinical history suspicious for COVID-19 infection, were characterized for SARS-CoV-2 presence, specific antigens expression and morphology, with the aim to investigate the possible direct effect of the virus in the onset of intra-abdominal venous thrombotic events.

Our results reported the presence of SARS-CoV-2 infection in all the samples analyzed (Figure 1A–D), with the highest levels found in patient 1 gallbladder and patient 2 colon in term of H-Score (Figure 2B). Interestingly, the comparison between patient 1 ileum and gallbladder

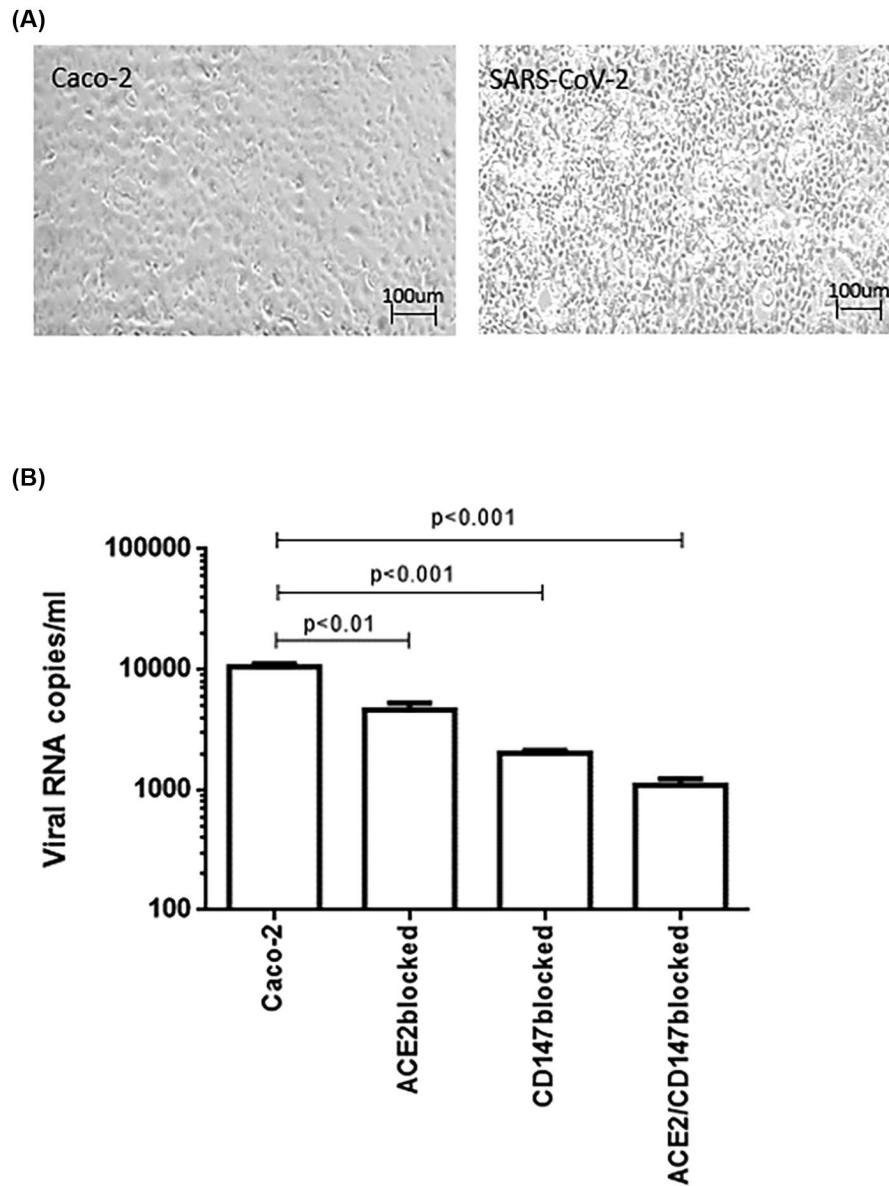


FIGURE 4 In vitro evaluation of SARS-CoV-2 infection of epithelial intestinal cells. (A) Caco-2 cell line was infected with SARS-CoV-2 at a multiplicity of infection (MOI) of 0.05 for 1 h at 37°C. Images of cells were captured with an optical microscope to detect the typical SARS-CoV-2-induced cytolitic effects. (B) Caco-2 cells were pre-treated with anti-ACE2 (ACE2 blocked) or anti-CD147 (CD147 blocked) moAbs and infected with SARS-CoV-2. Viral yield was quantified in the cell supernatant using quantitative reverse-transcription PCR (qRT-PCR). Data are representative of three independent experiments

revealed a different amount of viral infection (Figure 1B), which was significantly higher in gallbladder sample (Figure 2A,B), suggesting a different susceptibility of the two tissues. We evaluated the expression of ACE2 and CD147 surface molecules. ACE2 is the main SARS-CoV-2 receptor, while CD147 is considered a possible susceptibility factor for SARS-CoV-2 infection,¹⁶ expressed during pathological conditions in the lung, bowel tissues¹³ and during stroke.¹⁵

We observed a comparable expression of ACE2 receptor in all tissues (Figure 1E–H), except for patient 2 colon (Figure 1G). On the contrary, there is a differential

expression of the CD147 (Figure 1I–N). CD147 appeared to be highly expressed in patient 1 gallbladder (Figures 1L and 2A,D), where we also observed ACE2 expression. Patient 2 colon sample, despite the absence of ACE2 expression, presented a reliable expression of CD147 (Figure 1M) in the presence of a significant SARS-CoV-2 infection. These data suggest a possible involvement of CD147 in gastrointestinal SARS-CoV-2 infection, that might act in the presence of low levels of ACE2 expression. No significant difference was observed in MMP-9 expression (Figures 1O–R and 2A,E). In fact, despite CD147 induce MMP-9 expression⁴¹ and increased MMP-9 has

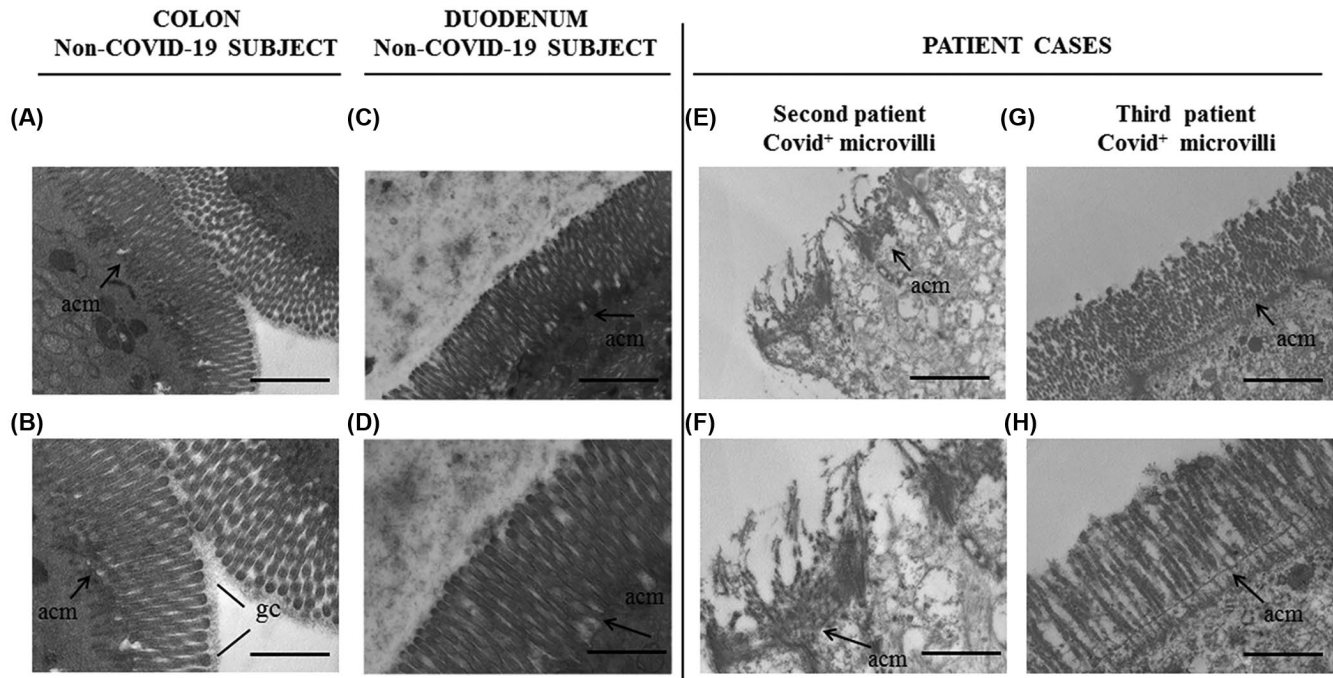


FIGURE 5 Morphology evaluation by TEM analysis. Representative TEM images of the epithelial cell apical surface microvilli of: (A and B): a colon of non-COVID-19 subject; (C and D): a duodenum of non-COVID-19 subject; (E and F): the colon of the second Covid+ patient; (G and H): the duodenum of the third Covid+ patient. Acm, apical cell membrane; gc, glycocalyx. Scale bars correspond to 2 μ m (A,C,E,G) and 1 μ m (B,D,F,H)

been associated to lung failure in COVID-19 patients,³⁰ MMP-9 was not found increased even in the presence of high CD147 expression.

Again, the expression of HLA-G in the presence of SARS-CoV-2 was reported in all the intestinal tissue samples, but not in patient 1 gallbladder sample (Figures 1S–V and 2A,F), where its lack was associated to a high CD147 expression. The modulation of HLA-G by SARS-CoV-2 in the gut as an immunoevasion mechanism has already been described previously³ and is in line with our results.

It could be hypothesized that the absence of HLA-G found in patient 1 gallbladder (Figure 1T) could derive by the shedding of HLA-G due to other MMPs induced by CD147,^{33,34} supporting once again a differential behaviour of viral infection in different tissues, mediated by a peculiar CD147 expression.

Moreover, the analysis of VEGF revealed an increased expression in the areas in which relevant SARS-CoV-2 presence was demonstrated, particularly considering patient 1 gallbladder (Figure 1 overlapping, Figure 2A,G), in association to consistent CD147 expression (Figure 1L). This data suggested that the onset of the thrombotic event during SARS-CoV-2 infection may involve VEGF via CD147, in line with previous data reporting CD147 involvement in VEGF modulation in pathological bowel conditions.¹⁴ Moreover, CD147 expression has been reported on vascular endothelium in the absence of ACE2, underlying the potential implication of this molecules in

the presence of vascular damages due to SARS-CoV-2 infection, independently from ACE2 presence.¹⁹

Our finding on SARS-CoV-2 SP binding-site on bowel tissue that co-localized with CD147 expression (Figure 3) is in line with previous results concerning CD147 engagement during viral infection^{16,17} and supported its role as a susceptibility factor in SARS-CoV-2 bowel infection and ischemia. As a proof of concept, the blocking of CD147 receptor decreased drastically SARS-CoV-2 infection in intestinal epithelial cells (Figure 4B).

Finally, the morphological profile analysis of tissues samples by TEM revealed the presence of microvilli with a significant shorter length, partially deepened beyond the acm and with an irregular gc distribution in patients 2 and 3 COVID-19 tissues, compared to the controls.

In conclusion, this work supported the existence of a peculiar pathogenic process for SARS-CoV-2 infection in the digestive tract of patients without any symptom attributable to typical COVID-19 disease but characterized by abdominal thrombosis. The hypothesis is that, since CD147 can regulate ACE2 levels and both molecules are affected by virus infection,¹⁷ the differential expression of CD147 observed along the digestive tract might determine a different tissue susceptibility to SARS-CoV-2 infection.

In fact, the highest extent of infection was reported in the presence of high CD147 expression, which was in turn associated with high VEGF levels, suggesting a possible role in thrombosis onset in this patient subset. Anyway,

due to the small number of subjects evaluated in this study, these data need to be confirmed in a larger group of samples.

ACKNOWLEDGMENTS

The authors thank Paola Boldrini (LTTA–Electron Microscopy Center, University of Ferrara, Italy), Cristina Bosi (Department of Translational Medicine, University of Ferrara, Italy) and Alessandro Sofia (University of Ferrara) for helpful collaboration.

DISCLOSURES

The authors declare that they have no conflicts of interest.

AUTHOR CONTRIBUTIONS

Daria Bortolotti and Carolina Simioni contributed equally to this article and both should be considered first author. Luca Maria Neri and Roberta Rizzo contributed equally to this article and both should be considered second author. Roberta Gafà and Angelina Passaro contributed equally to this article and both should be considered second author. Daria Bortolotti and Carolina Simioni wrote the first version of the paper. Angelina Passaro, Roberta Rizzo, and Luca Maria Neri also contributed to conception and design of the work. Roberta Rizzo, Luca Maria Neri and Angelina Passaro interpretation of the data and shared the first version of the paper. Carolina Simioni, Ilaria Laface and Gabriele Varano acquired images of biological samples in Transmission Electron Microscopy (TEM) and analyzed these data. Daria Bortolotti and Giovanna Schiuma, Sabrina Rizzo, Silvia Beltrami performed Immunohistochemical (IHC) analysis. Valentina Gentili performed SARS-CoV-2 infection of Caco-2 cell line and viral load quantitation. Savino Occhionorelli performed surgical intervention and specimen collection. Chiara Marina Semprini and Juana Maria Sanz collected biological samples and clinical data. Roberta Gafà performed the histopathological analysis and critically analyzed the images of IHC and TEM. Roberta Rizzo, Luca Maria Neri, Carolina Simioni, Daria Bortolotti, Chiara Marina Semprini, and Roberta Gafà acquired the images for the construction of the figures. Roberta Gafà performed the anatomo-histo-cytopathological diagnosis. All Authors contributed to literature search and revised the manuscript. Angelina Passaro is the corresponding author. She designed the study, coordinated the work of individual researchers or groups, made its own research funds available, assessed the quality of the data, and reviewed the manuscript. All authors approve the final version to be published. They are responsible for all aspects of the work and ensure its accuracy and integrity.

ORCID

Angelina Passaro  <https://orcid.org/0000-0001-8462-7000>

REFERENCES

- Burke RM, Midgley CM, Dratch A, et al. Active monitoring of persons exposed to patients with confirmed COVID-19 - United States, January-February 2020. *MMWR Morb Mortal Wkly Rep.* 2020;69:245-246.
- Loconsole D, Passerini F, Palmieri VO, et al. Recurrence of COVID-19 after recovery: a case report from Italy. *Infection.* 2020;48:965-967.
- Rizzo R, Neri LM, Simioni C, et al. SARS-CoV-2 nucleocapsid protein and ultrastructural modifications in small bowel of a 4-week-negative COVID-19 patient. *Clin Microbiol Infect.* 2021;27:936-937.
- Galan M, Jimenez-Altayo F. Small resistance artery disease and ACE2 in hypertension: a new paradigm in the context of COVID-19. *Front Cardiovasc Med.* 2020;7:588692.
- Yan T, Xiao R, Lin G. Angiotensin-converting enzyme 2 in severe acute respiratory syndrome coronavirus and SARS-CoV-2: a double-edged sword? *FASEB J.* 2020;34:6017-6026.
- Fu J, Zhou B, Zhang L, et al. Expressions and significances of the angiotensin-converting enzyme 2 gene, the receptor of SARS-CoV-2 for COVID-19. *Mol Biol Rep.* 2020;47:4383-4392.
- Evans JP, Liu S-L. Role of host factors in SARS-CoV-2 entry. *J Biol Chem.* 2021;297:100847.
- Wang K, Chen W, Zhang Z, et al. CD147-spike protein is a novel route for SARS-CoV-2 infection to host cells. *Signal Transduct Target Ther.* 2020;5:283.
- Chekol Abebe E, Mengie Ayele T, Tilahun Muche Z, Asmamaw Dejenie T. Neuropilin 1: a novel entry factor for SARS-CoV-2 infection and a potential therapeutic target. *Biol Targets Ther.* 2021;15:143-152.
- Ji K-Y, Kim S-M, Yee S-M, et al. Cyclophilin A is an endogenous ligand for the triggering receptor expressed on myeloid cells-2 (TREM2). *FASEB J.* 2021;35(4):e21479.
- Yurchenko V, Constant S, Eisenmesser E, Bukrinsky M. Cyclophilin-CD147 interactions: a new target for anti-inflammatory therapeutics. *Clin Exp Immunol.* 2010;160:305-317.
- Liu C, von Brunn A, Zhu D. Cyclophilin A and CD147: novel therapeutic targets for the treatment of COVID-19. *Med Drug Discov.* 2020;7:100056.
- Yurchenko V, Constant S, Bukrinsky M. Dealing with the family: CD147 interactions with cyclophilins. *Immunology.* 2006;117:301-309.
- Wang H, Ye J, Liu R, et al. Clinical significance of CD147 in children with inflammatory bowel disease. *Biomed Res Int.* 2020;2020:1-7.
- Jin R, Liu S, Wang M, Zhong W, Li G. Inhibition of CD147 attenuates stroke-associated pneumonia through modulating lung immune response in mice. *Front Neurol.* 2019;10:853.
- Helal MA, Shouman S, Abdelwaly A, et al. Molecular basis of the potential interaction of SARS-CoV-2 spike protein to CD147 in COVID-19 associated-lymphopenia. *J Biomol Struct Dyn.* 2020;26:1-11.
- Fenzia C, Galbiati S, Vanetti C, et al. SARS-CoV-2 entry: at the crossroads of CD147 and ACE2. *Cells.* 2021;10:1434.
- Shilts J, Crozier TWM, Greenwood EJD, Lehner PJ, Wright GJ. No evidence for basigin/CD147 as a direct SARS-CoV-2 spike binding receptor. *Sci Rep.* 2021;11:413.
- Zong J, Li Y, Du D, Liu Y, Yin Y. CD147 induces up-regulation of vascular endothelial growth factor in U937-derived foam

- cells through PI3K/AKT pathway. *Arch Biochem Biophys.* 2016;609:31-38.
20. Pamukçu B. Inflammation and thrombosis in patients with COVID-19: a prothrombotic and inflammatory disease caused by SARS coronavirus-2. *Anatol J Cardiol.* 2020;24:224-234.
 21. Meini S, Giani T, Tascini C. Intussusceptive angiogenesis in Covid-19: hypothesis on the significance and focus on the possible role of FGF2. *Mol Biol Rep.* 2020;47:8301-8304.
 22. Song P, Li W, Xie J, Hou Y, You C. Cytokine storm induced by SARS-CoV-2. *Clin Chim Acta.* 2020;509:280-287.
 23. Song CY, Xu J, He JQ, Lu YQ. Immune dysfunction following COVID-19, especially in severe patients. *Sci Rep.* 2020;10:15838.
 24. Saulle I, Vicentini C, Clerici M, Biasin M. Antigen presentation in SARS-CoV-2 infection: the role of class I HLA and ERAP polymorphisms. *Hum Immunol.* 2021;82:551-560.
 25. Bortolotti D, Gentili V, Rizzo S, Rotola A, Rizzo R. SARS-CoV-2 spike 1 protein controls natural killer cell activation via the HLA-E/NKG2A pathway. *Cells.* 2020;9:1975.
 26. Rizzo R, Bortolotti D, Bolzani S, Fainardi E. HLA-G molecules in autoimmune diseases and infections. *Front Immunol.* 2014;5:592.
 27. LeMaout J, Zafaranloo K, Le Danff C, Carosella ED. HLA-G up-regulates ILT2, ILT3, ILT4, and KIR2DL4 in antigen presenting cells, NK cells, and T cells. *FASEB J.* 2005;19:662-664.
 28. Rizzo R, Di Luca D. Human herpesvirus 6A and 6B and NK cells. *Acta Microbiol Immunol Hung.* 2018;65:119-125.
 29. Bortolotti D, LeMaout J, Trapella C, Di Luca D, Carosella ED, Rizzo R. *Pseudomonas aeruginosa* quorum sensing molecule N-(3-oxododecanoyl)-L-homoserine-lactone induces HLA-G expression in human immune cells. *Infect Immun.* 2015;83:3918-3925.
 30. Ueland T, Holter JC, Holten AR, et al. Distinct and early increase in circulating MMP-9 in COVID-19 patients with respiratory failure. *J Infect.* 2020;81:e41-e43.
 31. Nighot P, Al-Sadi R, Rawat M, Guo S, Watterson DM, Ma T. Matrix metalloproteinase 9-induced increase in intestinal epithelial tight junction permeability contributes to the severity of experimental DSS colitis. *Am J Physiol Liver Physiol.* 2015;309:G988-G997.
 32. Rizzo R, Trentini A, Bortolotti D, et al. Matrix metalloproteinase-2 (MMP-2) generates soluble HLA-G1 by cell surface proteolytic shedding. *Mol Cell Biochem.* 2013;381:243-255.
 33. Jouneau S, Khorasani N, De Souza P, et al. EMMPRIN (CD147) regulation of MMP-9 in bronchial epithelial cells in COPD. *Respirology.* 2011;16:705-712.
 34. Zeng H, Qiu Y, Qu Y, et al. Expression of CD147 in advanced non-small cell lung cancer correlated with cisplatin-based chemotherapy resistance. *Neoplasma.* 2011;58(5):449-454.
 35. Hasegawa K, Kudoh S, Ito T. Somatostatin receptor staining in FFPE sections using a ligand derivative dye as an alternative to immunostaining. *PLoS ONE.* 2017;12:e0172030.
 36. Montet X, Yuan H, Weissleder R, Josephson L. Enzyme-based visualization of receptor-ligand binding in tissues. *Lab Invest.* 2006;86:517-525.
 37. Rizzo S, Savastano MC, Bortolotti D, et al. COVID-19 ocular prophylaxis: the potential role of ozonated-oils in liposome eyedrop gel. *TVST J.* 2021;10(9):7.
 38. Sun J, Hemler MEE. Regulation of MMP-1 and MMP-2 production through CD147/extracellular matrix metalloproteinase inducer interactions. *Cancer Res.* 2001;61:2276-2281.
 39. Keshavarz P, Rafiee F, Kavandi H, Goudarzi S, Heidari F, Gholamrezaezhad A. Ischemic gastrointestinal complications of COVID-19: a systematic review on imaging presentation. *Clin Imaging.* 2020;73:86-95.
 40. Besutti G, Bonacini R, Iotti V, et al. Abdominal visceral infarction in 3 patients with COVID-19. *Emerg Infect Dis.* 2020;26:1926-1928.
 41. Suzuki S, Toyoma S, Kawasaki Y, Nanjo H, Yamada T. CD147 promotes invasion and MMP-9 expression through MEK signaling and predicts poor prognosis in hypopharyngeal squamous cell carcinoma. *Adv Clin Exp Med.* 2021;30:41-48.

SUPPORTING INFORMATION

Additional supporting information may be found in the online version of the article at the publisher's website.

How to cite this article: Bortolotti D, Simioni C, Neri LM, et al. Relevance of VEGF and CD147 in different SARS-CoV-2 positive digestive tracts characterized by thrombotic damage. *FASEB J.* 2021;35:e21969. doi:[10.1096/fj.202100821RRR](https://doi.org/10.1096/fj.202100821RRR)